Ann. Occup. Hyg., Vol. 56, No. 2, pp. 233–241, 2012

doi:10.1093/annhyg/mer103

Control of Cr^{6+} Emissions from Gas Metal Arc Welding Using a Silica Precursor as a Shielding Gas Additive

NATHAN TOPHAM[1], JUN WANG[1], MARK KALIVODA[1], JOYCE HUANG[1], KUEI-MIN YU[1], YU-MEI HSU[1,2], CHANG-YU WU[1]*, SEWON OH[3], KUK CHO[4,6] and KATHLEEN PAULSON[5]

[1]Department of Environmental Engineering Sciences, University of Florida, PO Box 116450, Gainesville, FL 32611-6450, USA; [2]Wood Buffalo Environmental Association, #100 - 330 Thickwood Boulevard, Ft. McMurray, Alberta T9K 1Y1, Canada; [3]Department of Civil and Environmental Engineering, Sangmyung University, San 98-20, Anseo-dong, Cheonan, Chungnam 330-720, Korea; [4]Korea Institute of Geoscience and Mineral Resources, 92 Gwahang-no, Yuseong-gu, Daejeon 305-350, Korea; [5]Naval Facilities Engineering Command, Engineering Service Center, NAVFAC ESC (EV21), 1100 23rd Street, Port Hueneme, CA 93043

Received 20 January 2011; in final form 24 August 2011; published online 21 November 2011

Hexavalent chromium (Cr^{6+}) emitted from welding poses serious health risks to workers exposed to welding fumes. In this study, tetramethylsilane (TMS) was added to shielding gas to control hazardous air pollutants produced during stainless steel welding. The silica precursor acted as an oxidation inhibitor when it decomposed in the high-temperature welding arc, limiting Cr^{6+} formation. Additionally, a film of amorphous SiO_2 was deposited on fume particles to insulate them from oxidation. Experiments were conducted following the American Welding Society (AWS) method for fume generation and sampling in an AWS fume hood. The results showed that total shielding gas flow rate impacted the effectiveness of the TMS process. Increasing shielding gas flow rate led to increased reductions in Cr^{6+} concentration when TMS was used. When 4.2% of a 30-lpm shielding gas flow was used as TMS carrier gas, Cr^{6+} concentration in gas metal arc welding (GMAW) fumes was reduced to below the 2006 Occupational Safety and Health Administration standard (5 $\mu g\ m^{-3}$) and the efficiency was >90%. The process also increased fume particle size from a mode size of 20 nm under baseline conditions to 180–300 nm when TMS was added in all shielding gas flow rates tested. SiO_2 particles formed in the process scavenged nanosized fume particles through intercoagulation. Transmission electron microscopy imagery provided visual evidence of an amorphous film of SiO_2 on some fume particles along with the presence of amorphous SiO_2 agglomerates. These results demonstrate the ability of vapor phase silica precursors to increase welding fume particle size and minimize chromium oxidation, thereby preventing the formation of hexavalent chromium.

Keywords: aerosol size distribution; hexavalent chromium; shielding gas; vapor phase sorbent; welding fume

INTRODUCTION

Gas metal arc welding (GMAW) is a commonly used process that uses mild or stainless steel wire as filler material to join pieces of metal. Shielding gas is used to protect the superheated weld site from gaseous species that degrade the weld's mechanical properties

*Author to whom correspondence should be addressed.
Tel: +1-352-392-0845; fax: +1-352-392-3076;
e-mail: cywu@ufl.edu
[6]Present address: School of Civil and Environmental Engineering, Pusan National University, 30 Jangjeon-dong, Geumjung-gu, Busan 609-735, Korea

and destabilize the welding arc. The operator controls welding parameters such as voltage, shielding gas composition, shielding gas flow rate, and wire feed speed to obtain desired weld characteristics. The operating parameters impact fume formation as well as weld characteristics, the complexity of which creates a challenge for the industry to balance maximum product quality with minimum emissions.

The intense energy of the welding process results in the formation of fumes containing a high number concentration of particles containing toxic metals as well as gaseous species including ozone and nitrogen oxides (Hewett, 1995b; Jenkins *et al.*, 2005; Liu *et al.*, 2007). Fume aerosols generated during arc welding are typically <1 μm in diameter and the primary particles are often in the nanometer range (Zimmer *et al.*, 2002; Biswas and Wu, 2005; Jenkins *et al.*, 2005). The fume characteristics are influenced by a variety of parameters, including shielding gas composition, welding wire composition, voltage, and metal transfer mode (Zimmer *et al.*, 2002; Hovde and Raynor, 2007).

Stainless steel welding fumes contain manganese and iron as well as chromium and nickel (Castner and Null, 1998; Heung *et al.*, 2007). About 1–5% of the chromium found in GMAW fumes is in the hazardous hexavalent state (Heung *et al.*, 2007; Serageldin and Reeves, 2009). These metals are layered in a core-shell structure that typically has a core made up primarily of iron with other metals making up the outer layers along with surface enrichment by lighter elements such as silicon, chlorine, and fluorine (Konarski *et al.*, 2003; Maynard *et al.*, 2004).

Welding uses a shielding gas to maintain arc stability, produce desirable weld penetration, and reduce fume formation rate (Dennis *et al.*, 1997; Ebrahimnia *et al.*, 2009). The shielding gas chosen has an impact on ultraviolet (UV) light, ozone generated, particle size distribution of aerosols, and the amount of Cr^{6+} (Dennis *et al.*, 1997; Zimmer *et al.*, 2002). The use of shielding gas in GMAW decreases overall fume formation rate; however, the formation rates of UV light, ozone, and Cr^{6+} all increased with shielding gas flow rate (Dennis *et al.*, 1997). Hexavalent chromium and ozone in welding fumes lead to many adverse health effects following occupational exposure (Antonini, 2003; Lillienberg *et al.*, 2008). Cr^{6+} is a known human carcinogen, with extensive human and animal data available (IARC, 1990). Studies of welding emissions in California found that welding is the primary source of airborne Cr^{6+} in the state (Chang *et al.*, 2004). Nickel is also a known human carcinogen (IARC, 1990), while manganese exposure can cause a number of adverse neurological effects, including a Parkinson's-like disorder known as manganism (Antonini *et al.*, 2006; Bowler *et al.*, 2006).

The aerodynamic diameter and shape of welding aerosols impact where welding fume particles deposit in the respiratory system and how rapidly the particles are cleared once deposited in the lungs. Few welding fume particles deposit in the upper respiratory system where clearance occurs rapidly. Welding fume particles deposit more readily in the lower regions of the respiratory system where clearance from the lungs is less effective (Hewett, 1995a; Yu *et al.*, 2000; Kleinstreuer *et al.*, 2008). Toxicity of nanoparticles is unique because the solid particles can be translocated across pathways other than the respiratory system that are typically not considered for larger particles (Biswas and Wu, 2005). For example, manganese nanoparticles can be translocated through the olfactory nerve directly to the brain where manganese expresses neurotoxic effects (Elder *et al.*, 2006). The soluble fraction of welding fumes is responsible for toxicity due to oxidative stress and free radical production (Taylor *et al.*, 2003; McNeilly *et al.*, 2004). Welding particles differ from other metal aerosols in that the insoluble and soluble fractions of the fumes are both significant contributors to toxicity (Antonini *et al.*, 2004).

Occupational Safety and Health Administration (OSHA) recently lowered the permissible exposure limit for Cr^{6+} in occupational air from 52 to 5 $\mu g \cdot m^{-3}$ (OSHA, 2006). The 2006 regulation included a 4-year extension until May 2010 for industry to install engineering controls to reduce exposures. This change placed pressure on industry to develop new control technologies to limit emissions of Cr^{6+} from arc welding. The simplest method of controlling welding fume exposure is removing the fumes from the breathing zone of the welder although preventing exposure to Cr^{6+} is preferred to evacuating the fumes using exhaust ventilation. High-velocity/low-volume local exhaust systems can reduce exposure to metals in welding fumes by about half if the hose for the pump is placed 5.1–7.6 cm (2–3 inches) from the welding torch (Meeker *et al.*, 2007). The use of reducing agents as shielding gas additives can reduce ozone formation in the welding fume (Dennis *et al.*, 2002). Similarly, the addition of reactive metals, such as zinc and aluminum, to welding wires can reduce Cr^{6+} formation (Dennis *et al.*, 1996). However, these technologies have not controlled formation of Cr^{6+} effectively enough to gain acceptance in industry. Hence, it is necessary to develop a control technology that will limit exposure to these pollutants while maintaining the integrity of the welded metal.

Sorbent injection into combustion systems has been examined as a means for removing trace metals. Sorbents are capable of scavenging a variety of metals in vapor phase in combustion systems to prevent nucleation of metallic aerosols (Biswas and Wu, 1998). Injection of bulk solid phase sorbents is not feasible for welding systems. Fortunately, vapor phase sorbent precursors have recently emerged as an alternative to solid phase materials. Previous research has shown that vapor phase silica precursor (e.g. tetraethyloxysilane) is capable of lowering Cr^{6+} emissions from gas tungsten arc welding (Topham *et al.*, 2010). Amorphous silica, formed from pyrolysis and subsequent oxidation of precursor chemicals, has been proven effective as a sorbent for lead produced during combustion. It is capable of forming an amorphous web that effectively captures ultrafine metal aerosols and increases their particle size (Owens and Biswas, 1996a,b; Biswas and Zachariah, 1997; Lee *et al.*, 2005). Amorphous silica may cause respiratory inflammation, emphysema, and other respiratory problems. However, epidemiological evidence does not suggest that amorphous silica persists in the respiratory system and causes cancer and fibrosis in the way that crystalline silica does (Reuzel *et al.*, 1991; Merget *et al.*, 2002). In this study, tetramethylsilane (TMS) was used as a shielding gas additive during GMAW to prevent formation of Cr^{6+}. The total shielding gas flow rate and the flow rate of TMS carrier gas were varied to investigate their effects on the efficacy of Cr^{6+} control and to determine the optimal feed conditions. Aerosol size distribution was monitored to assess the impact of TMS additive on resultant particle size, which has implications for subsequent respiratory deposition.

EXPERIMENTAL METHODS

The welding fume generation and sampling system (Fig. 1) followed a modified American Welding Society fume hood design (AWS, 1999). A conical chamber 91.4 cm (36 inches) in diameter at the base, 20.3 cm (8 inches) in diameter at the pump, and 91.4 cm (36 inches) in height was constructed. A Lincoln Power MIG 140C welder was used for producing welding fumes using ER 308L (0.09 cm diameter, 18 $g \cdot min^{-1}$ wire feed rate) stainless steel welding wire, which has an average chromium content of 19.5–22.0%. This wire also contains 9.0–11.0% Ni, 1.0–2.5% Mn, and 0.35–0.65% Si, according to its material safety data sheet. The sampling time, pump flow rate, and welding wire feed rate were kept constant throughout the experiment. This allows for conversion of the results, presented in micrograms Cr^{6+} per cubic meter, to micrograms Cr^{6+} per mass of welding wire consumed by multiplying the values presented by 0.07 (this value is derived by dividing the pump flow rate by the welding wire feed rate). Mild steel base metal was used for sampling in order to avoid interference from chromium emitted by the base sheet metal. The welder was operated in short-circuit mode with a contact tube working distance of ~1.9 cm (0.75 inches). The welding torch was modified to allow injection of TMS (CAS # 75-76-3) by inserting a Y-fitting to connect the torch and the gas hose. The wire guide was lengthened to ensure it was long enough to reach the contact tip. The trigger was removed and the wires inside the trigger were extended outside the chamber to allow remote operation of the welding gun. The welding gun used was a Lincoln Magnum 100L and the gas nozzle had an inner diameter of 0.95 cm (3/8 inches). The hose from the shielding gas cylinder was connected to a T-fitting to allow the gas flow to be split into two parts. The main shielding gas flow was passed through the welder as in normal operation while the remainder of the gas was used as the TMS carrier gas.

The recommended minimum shielding gas flow rate designated for this model of welder is 15 lpm (liters per minute). An initial shielding gas flow rate of 20 lpm was chosen to produce quality welds after preliminary testing demonstrated that this flow rate produced welds with good bead appearance and free of porosity upon visual inspection. The silica precursor feed rate was controlled by varying the flow rate of carrier gas that was passed over the liquid TMS reservoir, maintained at 0°C, with a mass flow controller. The carrier gas saturated with TMS vapor was then rejoined to the main shielding gas flow prior to reaching the welding torch. The base metal was placed on a rotating turntable (MK Products Aircrafter T-25) placed in the hood to maintain a constant weld speed. A 90-mm-diameter glass fiber filter (Millipore APFA 090) was placed at the top of the hood and connected to a high-volume [Hi-Vol; 1.27 $m^3 \cdot min^{-1}$ (45 $ft^3 \cdot min^{-1}$)] pump for collecting the aerosols. The sampling time was 85 s throughout the experiments. A mixture of 75% Ar and 25% CO_2 was used as the shielding gas, which acted as the needed carrier gas for TMS without requiring a secondary carrier gas. TMS is highly volatile with a vapor pressure at room temperature of 598 mmHg (Aston *et al.*, 1941). The TMS reservoir was placed in an ice bath to lower the vapor pressure (~270 mmHg at 0°C).

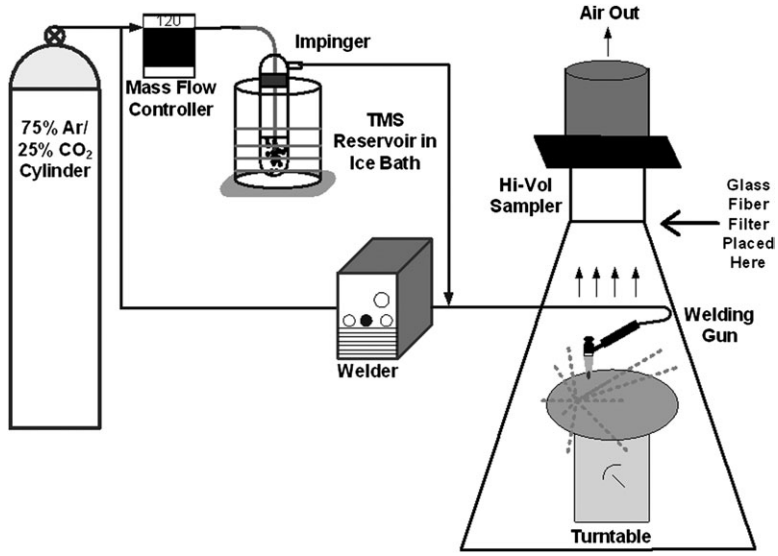

Fig. 1. GMAW fume generation and sampling system.

Baseline samples using 75% Ar and 25% CO_2 as a shielding gas (i.e. no flow going through the TMS reservoir) were run to determine emissions of Cr^{6+} during normal welding operation using short-circuit metal transfer. This scenario represents the standard welding method currently used in industrial environments. Experimental set A was performed using three TMS carrier gas flow rates (2.1, 4.2, and 6.3% of total shielding gas flow rate) at 20 lpm of total shield gas flow rate to determine the effect of TMS carrier gas flow rate on Cr^{6+} formation. In experimental set B, total shielding gas flow rate was increased to 25 lpm, and 5.0% of the shielding gas was used as TMS carrier gas. Experimental set C used a total shielding gas flow rate of 30 lpm and TMS carrier gas flow rates of 1.4, 2.8, 3.5, and 4.2%. Experimental sets B and C were performed to test the effect of shielding gas flow rate on the efficacy of this technology.

Ion chromatography (IC; Dionex ICS 1500, CS5A analytical column, DS6 conductivity detector) was used to measure the soluble hexavalent chromium species, chromate (CrO_4^{2-}). Sample extraction for IC followed a modified National Institute for Occupational Safety and Health (NIOSH) Method 7604 (NIOSH, 1994). The analytical column differs from the anionic column recommended in the NIOSH method. The manufacturer of the ion chromatograph recommends the cationic CS5A analytical column that is also capable of separating certain anionic species, such as chromate. The eluent chosen for the current study was sodium bicarbonate (5 mM) and sodium carbonate (1 mM) rather than the sodium bicarbonate and sodium hydroxide eluent used in the NIOSH method, as per manufacturer's specifications for the analytical column used in this study. Soluble Cr^{6+} species were extracted using the eluent and heated in a water bath to 100°C for 1 h. Additionally, transmission electron microscopy (TEM; Model 2010F; JEOL) was used to observe SiO_2 coating formed on fume particles and particle morphology. Specialty grids designed for TEM (Pelco, Lacey Carbon Type-A, 300 mesh) were directly loaded with fume particles for imaging. A scanning mobility particle sizer (SMPS; TSI Model 3081 Long DMA) was used to obtain aerosol size distribution data. For aerosol size distribution measurement, welding was performed for 10 s and stopped at which point the SMPS pump was turned on. After the SMPS completed its 135-s sampling run, the Hi-Vol pump was turned on to clear the chamber of particles. One-way analysis of variance (ANOVA) was conducted to verify difference among groups.

RESULTS AND DISCUSSION

20 lpm shielding gas flow rate

The impact of TMS addition on Cr^{6+} generation during GMAW using a total shielding gas flow rate of 20 lpm is shown in Fig. 2a (filled circles indicate data points). There was no statistically significant difference between the amount of Cr^{6+} mass concentration in the fumes regardless of the amount of TMS added ($P = 0.229$, ANOVA single factor, $\alpha = 0.05$). A large amount of white powder was observed on the

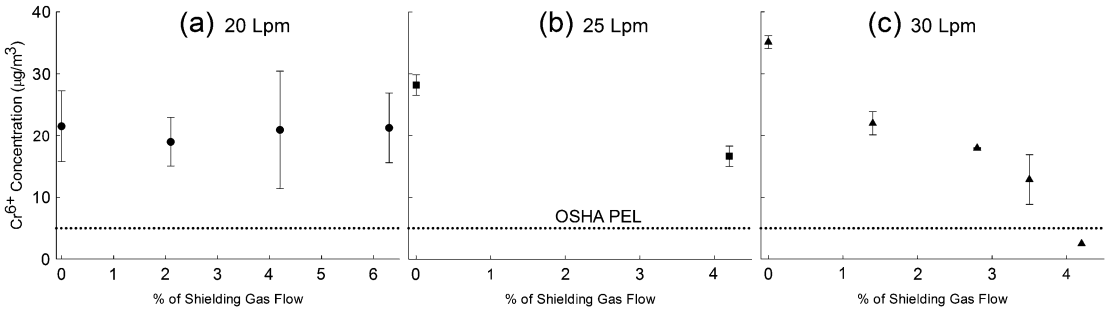

Fig. 2. Average Cr^{6+} mass concentration as a function of TMS carrier gas flow rate at (a) 20, (b) 25, and (c) 30 lpm total shielding gas flow rate. Baseline samples using no TMS are presented closest to the y-axis in each figure. The values on the x-axis denote how much of the total shielding gas flow rate is used as TMS carrier gas. The data point to the far right of (c) has no error bar because all samples were below the detection limit.

Fig. 3. Head of the welding torch gas nozzle (inner diameter = 0.97 cm) after sampling showing white powder from premature decomposition of TMS using 20 lpm of welding shielding gas.

head of the welding torch after sampling (Fig. 3). It likely resulted from premature thermal decomposition of TMS inside the head of the welding torch. When this happened, TMS did not function as an effective oxidation inhibitor or coat fume particles in a SiO_2 film because the TMS had already reacted before reaching the area where fume particle formation was occurring.

The addition of TMS led to an increase in fume particle size as shown in Fig. 4a. During baseline welding, a large number of particles with a mode size of ~18 nm were observed by SMPS measurements. As increasing amounts of TMS were added, this peak decreased and eventually vanished when 6.3% TMS was added. The particle size distribution shifted toward larger particles with the nanoparticles being replaced with particles >100 nm in diameter.

25 lpm shielding gas flow rate

There was an increase in baseline Cr^{6+} mass concentration when the shielding gas flow rate was increased from 20 to 25 lpm (Fig. 2b; filled squares indicate data points). When 5.0% of the shielding gas flow rate was used as TMS carrier gas, there was a significant decrease in Cr^{6+} concentration of ~40% with a P value far below 0.05 (Student's T-test, two tails, unequal variance). The reduction in Cr^{6+} indicated that some of the TMS was surviving until reaching the area where reactive oxygen species were present. After sampling, there was still some white powder observed inside the head of the welding torch, although not as much as in the 20-lpm case.

The SMPS particle size data for 25 lpm shielding gas flow rate followed the same pattern as that for 20 lpm, as displayed in Fig. 4b. When welding without TMS, a large peak was seen at ~20 nm. As TMS feed rate was increased, the peak in the nanometer size range shrank relative to the peak >100 nm.

30 lpm shielding gas flow rate

The results indicate adding TMS to shielding gas of 30 lpm reduced formation of Cr^{6+}, as seen in Fig. 2c (filled triangles indicate data points). When 4.2% of the shielding gas was used as TMS carrier gas, the Cr^{6+} concentration was successfully reduced to below the IC detection limit for all replicate samples. For display purpose, the concentration for all non-detectable samples was set equal to the detection limit. This was a reduction in Cr^{6+} concentration of at least 93% compared to baseline conditions. There was not as

much white powder inside the head of welding torch as observed in the 20-lpm case. The reduction in Cr^{6+} concentration achieved when using TMS as a shielding gas additive exceeded the results seen in previous studies that incorporated reducing agents into shielding gas or welding wire (Dennis *et al.*, 1996, 2002; Topham *et al.*, 2010). The differences in Cr^{6+} mass among TMS feed rates were statistically significant ($P = 6.8 \times 10^{-11}$, ANOVA single factor, $\alpha = 0.05$).

As increasing amounts of TMS were fed into the system, the metal nanoparticles were scavenged by SiO_2 agglomerates and the particle size distribution shifted toward larger particle sizes (Fig. 4c). The count mode diameter increased from 18 nm in the nanometer

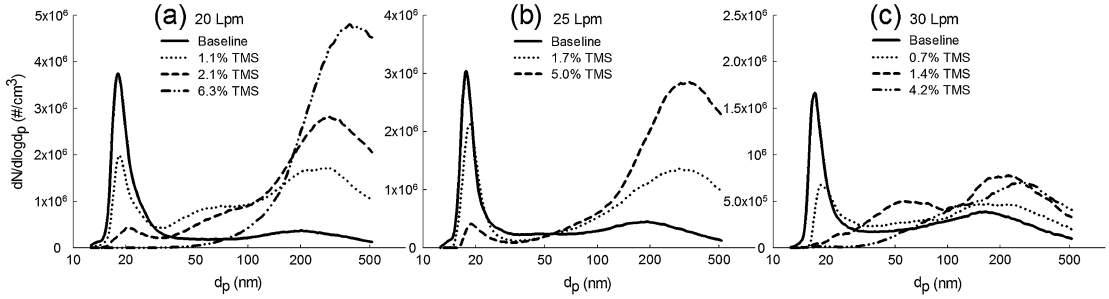

Fig. 4. GMAW fume particle size distributions at (a) 20, (b) 25, and (c) 30 lpm shielding gas flow rate. Note: total particle number concentration decreased as shielding gas flow rate increased.

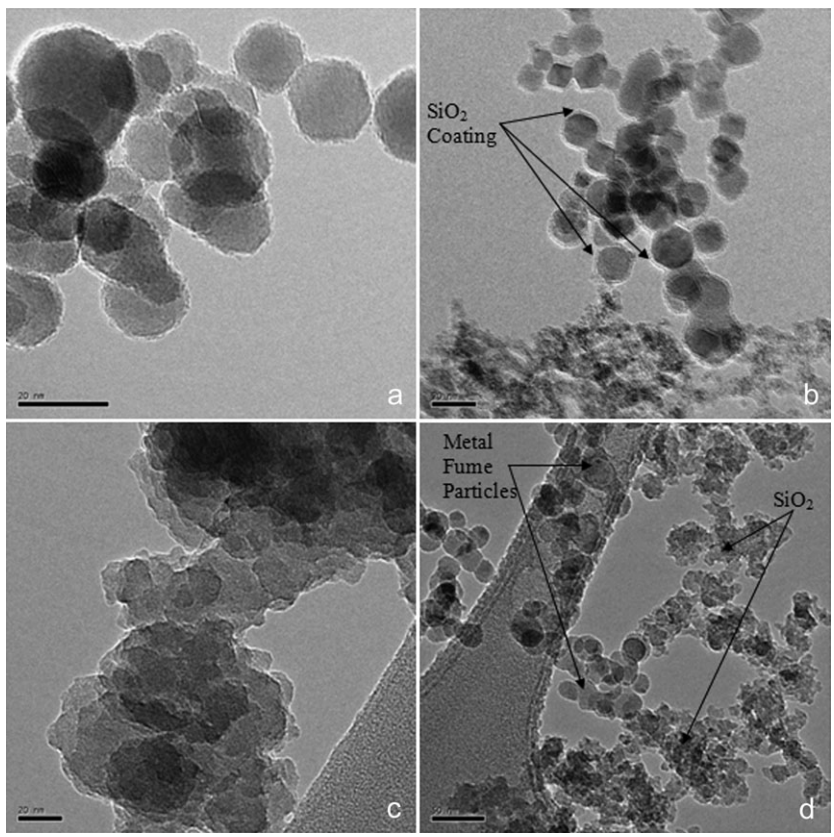

Fig. 5. TEM images of welding fume particles collected at 4.2% of TMS carrier gas flow rate with 30 lpm of total shielding gas flow rate: (a) GMAW fume agglomerate without SiO_2 coating (scale = 20 nm); (b) GMAW fume agglomerate with SiO_2 coating indicated by arrows (scale = 20 nm); (c) amorphous SiO_2 agglomerate (scale = 20 nm); (d) metal-SiO_2 agglomerate formed by intercoagulation (scale = 50 nm).

range to 270 nm as TMS feed rate was increased to 4.2%. The increase in particle size observed when TMS was added agreed with previous studies that utilized silica precursors to control lead emissions from combustion systems. In those studies, adding silica precursors increased particle size out of the nanometer range (Owens and Biswas, 1996a,b).

TEM images were obtained to determine whether a SiO_2 coating was present on fume particles when 4.2% TMS was used as an additive. For baseline samples without TMS feed (Fig. 5a), the images show metal nanoparticles without SiO_2 coating. Careful examination of Fig. 5a reveals that some surface enrichment with lighter elements did occur, which mirrors results of previous studies of welding fume particle structure exhibiting surface enrichment with silicon, chlorine, and fluorine (Maynard *et al.*, 2004). With TMS feed, Fig. 5b shows an agglomerate particle that had a coating of SiO_2 encapsulating the entire agglomerate rather than surface enrichment of individual primary particles. The coating in Fig. 5b was more significant than the surface enrichment seen on individual primary particles under baseline conditions in previous research (Konarski *et al.*, 2003; Maynard *et al.*, 2004). Meanwhile, not all silica formed in the process ended up as the coating; Fig. 5c displays an agglomerate particle made up of amorphous SiO_2. There are also agglomerates of metal fume particles with amorphous SiO_2 particles, as shown in Fig. 5d. This result is consistent with previous research demonstrating that intercoagulation can scavenge nanoparticles (Lee and Wu, 2005). This is also echoed by the shift in mode size shown in Fig. 4. Twenty-nanometer particles have high deposition efficiency in the alveolar area (~50%), while 300-nm particles have the minimum deposition efficiency in the respiratory system (<15% for total deposition and <8% for alveolar deposition) (ICRP, 1994). Size increase out of the nanometer range to reduce respiration deposition, as shown, may be another potential benefit of the TMS process though full characterization of the impact of particle size shift on health effects is needed to validate the benefits.

The TEM images obtained show that coating by SiO_2 was not uniform for all fume particles. Some particles were not coated, some agglomerate particles were covered in a thin layer of SiO_2, and some separate amorphous agglomerates composed mostly of SiO_2 were also present. Figure 5b indicates that silica precursor additives can possibly encapsulate all types of metals in welding fume particles through the formation of a SiO_2 film on metal particles. This phenomenon is similar to that observed in previous research where metal nanoparticles formed in combustion systems can be trapped in a web of amorphous SiO_2 (McMillin *et al.*, 1996; Owens and Biswas, 1996a; Biswas *et al.*, 1997). Metal nanoparticles that are coated in SiO_2 may take longer to exhibit toxic effects because the SiO_2 coating could take weeks to dissolve in the respiratory system (Roelofs and Vogelsberger, 2004). This would provide the respiratory system's removal mechanisms more time to remove the particles before exposure to the toxic metals occurs. Indeed, Yu *et al.* (2010) showed significant reduction in biotoxicity of welding fume particles tested with *Escherichia coli* when TMS was added to the shielding gas, and amorphous silica produced in such a process was demonstrated to possess no biotoxicity to the bacteria. Meanwhile, the results also indicate that process optimization is needed to further lower the toxicity by more complete coverage, which will also lead to reduced consumption of TMS. Comparing the baseline results (i.e. no TMS) of all shielding gas flow rates, it can be seen that Cr^{6+} concentration increased as shielding gas flow rate increased, which is in agreement with prior studies (Dennis *et al.*, 1997). By avoiding premature decomposition, high shielding gas flow rate yielded better Cr^{6+} reduction when TMS process was adopted. Hence, measures to ensure proper timing of TMS decomposition will allow more effective amorphous silica coverage with more efficient utilization of TMS.

The shield gas flow rates used in this study were within the normal range of operation for the welding machine used. However, an optimized delivery system is necessary to transition this technology use in industrial settings. The modifications required to the shield gas system and laboratory equipment used in this study may present operational or safety concerns in an industrial setting. Some of the process parameters, such as the use of carbon steel plate, the shield gas mixture chosen, and the working distance chosen, may have introduced some error into the data. For example, stainless steel sheet metal would contribute some Cr^{6+} to the welding fumes. The error introduced from these variables could be eliminated through process optimization; however, any error would be relatively consistent across the samples in this study.

CONCLUSIONS

Silica precursors led to reduction in Cr^{6+} in GMAW fumes of >90% when 4.2% of the shielding gas was used to carry TMS at 30 lpm total shielding gas flow rate. The use of TMS as a shielding gas

additive greatly brought Cr^{6+} concentration down from a level that exceeded the OSHA permissible exposure limit to within regulatory limits. This result may help industry keep pace with tightening occupational limits for this hazardous air pollutant. The increase in particle size observed when TMS was added may be another benefit for using these chemicals. Further research to evaluate whether the increase in particle size achieved using TMS could help personal protective equipment protect workers from welding fume particles by reducing penetration through filters is desired. New technologies to scavenge nanoparticles from effluent gas streams will be required as nanomaterial manufacturing spreads. Silica precursors may provide a tool for dealing with this challenging problem. TEM imagery demonstrated that some particles were coated in a film of amorphous SiO_2. All of the metals contained in the particles that were coated in SiO_2 were insulated regardless of speciation.

More research is needed to determine whether this technology alters the toxic effects of welding fume particles containing nickel and manganese through encapsulation in amorphous silica. Further research is also necessary to verify that using silica precursors as shielding gas additives has no adverse effects on the mechanical properties of the materials being welded.

FUNDING

This work was supported by the U.S. Department of Defense through the Environmental Security Technology Certification Program (Project No. WP-0903) and General Research Project of the Korea Institute of Geoscience and Mineral Resources (KIGAM) funded by the Ministry of Knowledge and Economy (R543).

Acknowledgements—The authors would like to thank Drs Daniel P. Chang, Ian Kennedy, and Peter Kelly at the University of California-Davis for developing the initial idea of using silica precursors as shielding gas additives. The authors also acknowledge the Major Analytical Instrumentation Center at the University of Florida for assisting with TEM imagery.

REFERENCES

Antonini JM. (2003) Health effects of welding. Crit Rev Toxicol; 33: 61.

Antonini JM, Santamaria AB, Jenkins NT *et al*. (2006) Fate of manganese associated with the inhalation of welding fumes: potential neurological effects. Neurotoxicology; 27: 304–10.

Antonini JM, Taylor MD, Zimmer AT *et al*. (2004) Pulmonary responses to welding fumes: role of metal constituents. J Toxicol Environ Health A; 67: 233–49.

Aston JG, Kennedy RM, Messerly GH. (1941) The heat capacity and entropy, heats of fusion and vaporization and the vapor pressure of silicon tetramethyl. J Am Chem Soc; 63: 2343–8.

AWS. (1999) Method F1.2-1999-Laboratory method for measuring fume generation rates and total fume emission of welding and allied processes. Miami, FL: ANSI/AWS.

Biswas P, Wu CY. (1998) Control of toxic metal emissions from combustors using sorbents: a review. J Air Waste Manag Assoc; 48: 113–27.

Biswas P, Wu CY. (2005) Nanoparticles and the environment—a critical review. J Air Waste Manag Assoc; 55: 708–46.

Biswas P, Wu CY, Zachariah MR *et al*. (1997) Characterization of iron oxide-silica nanocomposites in flames, Part II: comparison of a discrete-sectional model predictions to experimental data. J Mater Res; 12: 714–23.

Biswas P, Zachariah MR. (1997) In situ immobilization of lead species in combustion environments by injection of gas phase silica sorbent precursors. Environ Sci Technol; 31: 2455–63.

Bowler RM, Gysens S, Diamond E *et al*. (2006) Manganese exposure: neuropsychological and neurological symptoms and effects in welders. Neurotoxicology; 27: 315–26.

Castner HR, Null TW. (1998) Chromium, nickel and manganese in shipyard welding fumes. Weld J; 77: 223s–31s.

Chang DP, Heung W, Yun M *et al*. (2004) Improving welding toxic metal emission estimates in California. Sacramento, CA.

Dennis JH, French MJ, Hewitt PJ *et al*. (1996) Reduction of hexavalent chromium concentration in fumes from metal cored arc welding by addition of reactive metals. Ann Occup Hyg; 40: 339–44.

Dennis JH, French MJ, Hewitt PJ *et al*. (2002) Control of exposure to hexavalent chromium and ozone in gas metal arc welding of stainless steels by use of a secondary shield gas. Ann Occup Hyg; 46: 43–8.

Dennis JH, Mortazavi SB, French MJ *et al*. (1997) The effects of welding parameters on ultra-violet light emissions, ozone and CrVI formation in MIG welding. Ann Occup Hyg; 41: 95–104.

Ebrahimnia M, Goodarzi M, Nouri M *et al*. (2009) Study of the effect of shielding gas composition on the mechanical weld properties of steel ST 37-2 in gas metal arc welding. Mater Des; 30: 3891–5.

Elder A, Gelein R, Silva V *et al*. (2006) Translocation of inhaled ultrafine manganese oxide particles to the central nervous system. Environ Health Perspect; 114: 1172–8.

Heung W, Yun M-J, Chang DPY *et al*. (2007) Emissions of chromium (VI) from arc welding. J Air Waste Manag Assoc; 57: 252–60.

Hewett P. (1995a) Estimation of regional pulmonary deposition and exposure for fumes from SMAW and GMAW mild-steel and stainless-steel consumables. Am Ind Hyg Assoc J; 56: 136–42.

Hewett P. (1995b) The particle size distribution, density and specific surface area of welding fumes from SMAW and GMAW mild-steel and stainless-steel consumables. Am Ind Hyg Assoc J; 56: 128–35.

Hovde CA, Raynor PC. (2007) Effects of voltage and wire feed speed on welding fume characteristics. J Occup Environ Hyg; 4: 903–12.

IARC. (1990) Chromium, nickel and welding. IARC monographs on the evaluation of carcinogenic risk of chemicals to humans. Lyon, France.

ICRP. (1994) Human respiratory tract model for radiological protection. Report No. Publication 66; Ann ICRP 24 (1–3). Tarrytown, NY: International Commission on Radiological Protection.

Jenkins NT, Pierce WMG, Eagar TW. (2005) Particle size distribution of gas metal and flux cored arc welding fumes. Weld J; 84: 156s–63s.

Kleinstreuer C, Zhang Z, Li Z. (2008) Modeling airflow and particle transport/deposition in pulmonary airways. Respir Physiol Neurobiol; 163: 128–38.

Konarski P, Iwanejko I, Cwil M. (2003) Core-shell morphology of welding fume micro- and nanoparticles. Vacuum; 70: 385–9.

Lee M-H, Cho K, Shah AP *et al*. (2005) Nanostructured sorbents for capture of cadmium species in combustion environments. Environ Sci Technol; 39: 8481–9.

Lee SR, Wu CY. (2005) Size distribution evolution of fine aerosols due to inter-coagulation with coarse aerosols. Aerosol Sci Technol; 39: 358–70.

Lillienberg L, Zock JP, Kromhout H *et al*. (2008) A population-based study on welding exposures at work and respiratory symptoms. Ann Occup Hyg; 52: 107–15.

Liu HH, Wu YC, Chen HL. (2007) Production of ozone and reactive oxygen species after welding. Arch Environ Contam Toxicol; 53: 513–8.

Maynard AD, Ito Y, Arslan I *et al*. (2004) Examining elemental surface enrichment in ultrafine aerosol particles using analytical scanning transmission electron microscopy. Aerosol Sci Technol; 38: 365–81.

McMillin BK, Biswas P, Zachariah M. (1996) In situ diagnostics of vapor phase growth of iron oxide-silica nanocomposites, Part I: 2-D planar laser-induced fluorescence and MIE imaging. J Mater Res; 11: 1552–61.

McNeilly JD, Heal MR, Beverland IJ *et al*. (2004) Soluble transition metals cause the pro-inflammatory effects of welding fumes in vitro. Toxicol Appl Pharmacol; 196: 95–107.

Meeker JD, Susi P, Flynn MR. (2007) Manganese and welding fume exposure and control in construction. J Occup Environ Hyg; 4: 943–51.

Merget R, Bauer T, Küpper HU *et al*. (2002) Health hazards due to the inhalation of amorphous silica. Arch Toxicol; 75: 625–34.

NIOSH. (1994) Method 7604: chromium, hexavalent by ion chromatography. Atlanta, GA.

OSHA. (2006) Chromium VI. 29 CFR 1910–1026. Washington, DC.

Owens TM, Biswas P. (1996a) Reactions between vapor phase lead compounds and in situ generated silica particles at various lead-silicon feed ratios: applications to toxic metal capture in combustors. J Air Waste Manag Assoc; 46: 530–8.

Owens TM, Biswas P. (1996b) Vapor phase sorbent precursors for toxic metal emissions control from combustors. Ind Eng Chem Res; 35: 792–8.

Reuzel P, Bruijntjes J, Feron V *et al*. (1991) Subchronic inhalation toxicity of amorphous silicas and quartz dust in rats. Food Chem Toxicol; 29: 341–54.

Roelofs F, Vogelsberger W. (2004) Dissolution kinetics of synthetic amorphous silica in biological-like media and its theoretical description. J Phys Chem B; 108: 11308–16.

Serageldin M, Reeves DW. (2009) Development of welding emission factors for Cr and Cr(VI) with a confidence level. J Air Waste Manag Assoc; 59: 619–26.

Taylor MD, Roberts JR, Leonard SS *et al*. (2003) Effects of welding fumes of differing composition and solubility on free radical production and acute lung injury and inflammation in rats. Toxicol Sci; 75: 181–91.

Topham N, Kalivoda M, Hsu YM *et al*. (2010) Reducing Cr^{6+} emissions from gas tungsten arc welding using a silica precursor. J Aerosol Sci; 41: 326–30.

Yu IJ, Kim KJ, Chang HK *et al*. (2000) Pattern of deposition of stainless steel welding fume particles inhaled into the respiratory systems of Sprague-Dawley rats exposed to a novel welding fume generating system. Toxicol Lett; 116: 103–11.

Yu K-M, Topham N, Wang J *et al*. (2010) Decreasing biotoxicity of fume particles produced in welding process. J Hazard Mater; 185: 1587–91.

Zimmer AT, Baron PA, Biswas P. (2002) The influence of operating parameters on number-weighted aerosol size distribution generated from a gas metal arc welding process. J Aerosol Sci; 33: 519–31.